35th Annual International Conference of the IEEE EMBS
Osaka, Japan, 3 - 7 July, 2013

Real-time high-resolution vascular ultrasound using frequency domain interferometry with the ROI-division process*

Hirofumi Taki, *Member, IEEE*, Takuya Sakamoto, *Member, IEEE*, Kousuke Taki, Makoto Yamakawa, *Member, IEEE*, Tsuyoshi Shiina, *Member, IEEE*, Motoi Kudo, *Member, IEEE*, and Toru Sato, *Member, IEEE*

Abstract— **We have proposed a high-range-resolution ultrasound imaging method for human carotid artery using an adaptive beamforming technique based on frequency domain interferometry (FDI). The method assumes that the received signal consists of multiple echoes of targets and noise, where the waveform of each echo is similar to that of the reference signal. In this study, we examine the dependence of the echo waveform on the target depth, and investigate the proper measurement-range for the FDI imaging method using a reference signal. Furthermore, we propose a ROI-division process, where each sub-ROI has a proper measurement-range for the application of the FDI imaging method. Simulation and experimental results show the efficiency of the ROI-division process in improving the image quality of human carotid artery acquired using the FDI imaging method. We believe that the modified FDI imaging method with the ROI-division process has the potential to facilitate significant progress in the detection of vessel stenosis and in the assessment of cardiovascular disease risk.**

I. Introduction

Cardiovascular disease is currently the leading cause of mortality. Since vascular ultrasound is one of the primary imaging modalities for the detection of vessel stenosis and for the investigation of cardiovascular disease risk [1], [2], the improvement of range resolution in vascular ultrasound is strongly desired.

Adaptive beamforming algorithms have been reported to acquire high-spatial-resolution images [3], [4]. Several researchers have applied adaptive beamforming algorithms to ultrasound imaging [5]–[8]; however, they solely focused on the improvement in lateral resolution.

*This work was partly supported by the Innovative Techno-Hub for Integrated Medical Bio-imaging Project of the Special Coordination Funds for Promoting Science and Technology, from the Ministry of Education, Culture, Sports, Science and Technology (MEXT), Japan and by MEXT/JSPS KAKENHI Grant Number 24592513.

H. Taki, T. Sakamoto and T. Sato are with the Graduate School of Informatics, Kyoto University, Yoshida-honmachi, Sakyo-ku, Kyoto 606-8501, Japan (e-mail: htaki@i.kyoto-u.ac.jp; t-sakamo@i.kyoto-u.ac.jp; sato.toru.6e@kyoto-u.ac.jp).

K. Taki and M. Kudo are with the Department of Anatomy, Shiga University of Medical Science, Seta Tsukinowa-cho, Otsu City, Shiga 520-2192, Japan (e-mail: taki@belle.shiga-med.ac.jp; kudo@belle.shiga-med.ac.jp).

M. Yamakawa is with the Advanced Biomedical Engineering Research Unit, Kyoto University, Yoshida-honmachi, Sakyo-ku, Kyoto 606-8501, Japan (e-mail: yamakawa.makoto.6x@kyoto-u.ac.jp).

T. Shiina is with the Graduate School of Medicine, Kyoto University, Yoshida-honmachi, Sakyo-ku, Kyoto 606-8501, Japan (e-mail: shiina@hs.med.kyoto-u.ac.jp).

The high-range-resolution imaging of carotid arterial walls should improve the accuracy in measuring carotid stiffness and carotid intima-media thickness (CIMT), where these indicators are commonly used to assess the risk of cardiovascular diseases. We have proposed a high-range-resolution ultrasound imaging method based on frequency domain interferometry (FDI) with the Capon method, an adaptive beamforming technique [9]–[12]. The method assumes that the received signal consists of multiple echoes of targets and noise, where the waveform of each echo is similar to that of the reference signal. However, previous studies have neglected to consider the dependence of the echo waveform on the target depth.

In this study, we examine the dependence of the echo waveform on the target depth, and investigate the proper measurement-range for the FDI imaging method using a reference signal. Furthermore, we propose a process, where each sub-ROI has a proper measurement-range for the application of the FDI imaging method. We explain the ultrasound imaging method with the proposed ROI-division process, and discuss the obtained results.

II. Materials and Methods

The proposed method is based on FDI with the Capon method. In this section, we briefly describe the signal processing based on FDI with the Capon method, and subsequently explain the variation in echo waveform caused by varying target depth. Finally, we report on the ROI-division process for suppressing the degradation of image quality caused by varying target depth.

A. Ultrasound Imaging Method Based on FDI with the Capon Method

The FDI imaging method employs phase compensation to coherently integrate the frequency components of the echo from the desired depth. The estimated intensity at a depth using the FDI method is given by

$$P = yy^{*} = \mathbf{W}^{T*}\mathbf{R}\mathbf{W}, \tag{1}$$

$$y = \mathbf{X}^{T}\mathbf{W}^{*}, \tag{2}$$

$$\mathbf{R} = \mathbf{X}\mathbf{X}^{T*}, \tag{3}$$

where $\mathbf{X}$ is the set of frequency components of a received signal after the delay and sum process, $\mathbf{R}$ is the correlation matrix of a received signal, and $\mathbf{W}$ is a weighting vector to compensate the phase of the frequency components [10].

We apply the Capon method to select an appropriate weighting vector. The Capon method suppresses the contribution of the echoes returned from targets of undesired depths, under the condition of a constant response at the desired depth. This problem is expressed as follows:

$$\min \quad P' = \mathbf{W}'^{\mathrm{T}*} \mathbf{R}_{\mathrm{A}} \mathbf{W}' \quad \text{subject to} \quad \mathbf{C}^{\mathrm{T}*} \mathbf{W}' = 1, \tag{4}$$

$$\mathbf{C} = [\exp(\mathrm{j}k_1 r) \quad \cdots \quad \exp\{\mathrm{j}k_N r\}]^{\mathrm{T}}, \tag{5}$$

where $\mathbf{R}_{\mathrm{A}}$ is the correlation matrix of a received signal after frequency averaging, k_n is the n-th wave number of frequency components of a received signal, N is the size of the correlation matrix $\mathbf{R}_{\mathrm{A}}$ and $r/2$ is the desired depth [10].

The estimated intensity of the FDI imaging method employing an appropriate weighting vector is given by

$$P_{\mathrm{Cap}}(r) = \frac{1}{\mathbf{C}^{\mathrm{T}*} (\mathbf{R}_{\mathrm{A}} + \eta' \mathbf{E})^{-1} \mathbf{C}}, \tag{6}$$

where $\eta'\mathbf{E}$ is a diagonal loading matrix used to avoid the instability in calculating the inverse matrix $\mathbf{R}_{\mathrm{A}}^{-1}$ [10].

B. Deterioration of Image Quality Caused by Varying Target Depth

The FDI imaging method with the Capon method assumes that the waveform of each echo is similar to that of the reference signal. However, the carotid ultrasound imaging is in near field conditions, and the echo waveform depends on the target depth. In previous studies the dependence of the echo waveform on the target depth was neglected, and thus varying target depth caused deterioration in image quality.

Fig. 1 shows the echo waveforms of horizontal interfaces at depths of 11, 13, 15, 17 and 19 mm in a simulation study. The aperture size of a linear array is 8 mm, the transmit center frequency is 7.5 MHz, the transmit focus is fixed to 15 mm and dynamic focusing is utilized for receive beamforming. Fig. 2 shows the estimated intensity acquired using the FDI imaging method, where the reference signal is the echo from a horizontal interface at a depth of 15 mm. In all cases, the method succeeds in estimating the interface depth; however, a false peak appears when the target depth is 11 mm. This false peak is mainly caused by disagreement at the latter part of the echo waveform between the echo of the 11-mm-depth interface and the reference signal.

C. FDI Imaging Method with the ROI-Division Process

We employ the ROI-division process (RDP) to suppress the disagreement between the waveform of an echo and that of the reference signal. Fig. 3 shows sub-ROIs divided from a ROI in a human carotid artery using RDP. Since the employment of RDP decreases the measurement range of each sub-ROI, the FDI imaging method can acquire a high-range-resolution image of each sub-ROI. We reconstruct the whole image of the ROI from the images of the sub-ROIs.

Fig. 4 shows the –6 dB range width of the FDI images for horizontal interfaces at depths of 11 to 19 mm in a simulation study. The FDI imaging method employs one of the echoes returned from the horizontal interfaces at depths of 12, 15 and 18 mm as the reference signal. When the depth of an interface is close to that of the reference signal, a sharp peak appears at the interface depth. The performance of the FDI imaging method using the reference signal at a depth of 15 mm has adequate beamwidth for all depths; however, a false peak accompanies the image of the interface at the depth of 11 mm, as shown in Fig. 5.

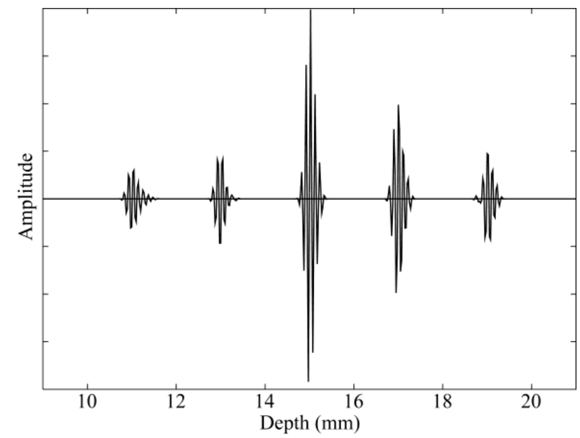

Figure 1. Echo waveformes of horizontal interfaces at depths of 11, 13, 15, 17 and 19 mm.

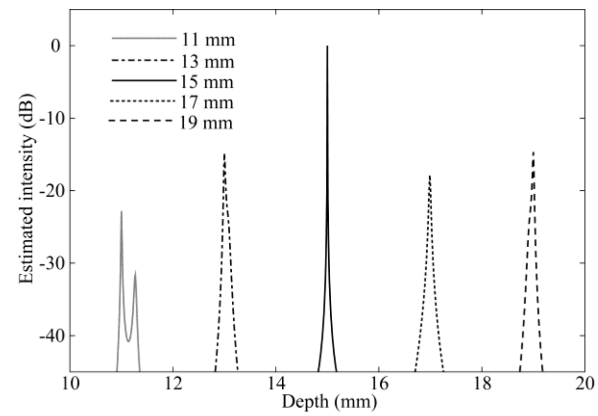

Figure 2. Estimated intensity acquired using a conventional FDI imaging method. A single interface exists at depths of 11, 13, 15, 17 and 19 mm, and the conventional FDI imaging method employs an echo returned from a horizontal interface at a depth of 15 mm as the reference signal.

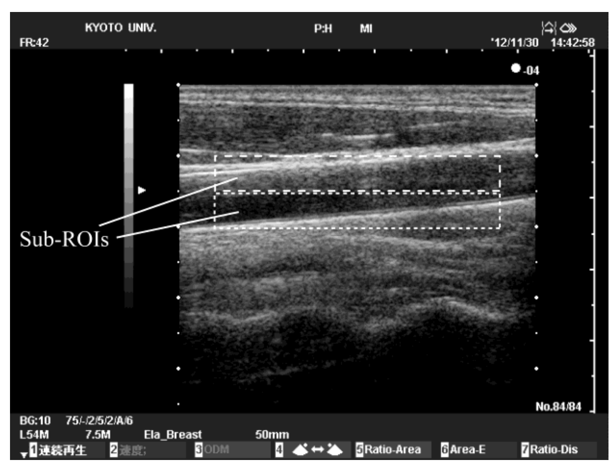

Figure 3. Sub-ROIs divided from a ROI in a human carotid artery using the ROI-division process.

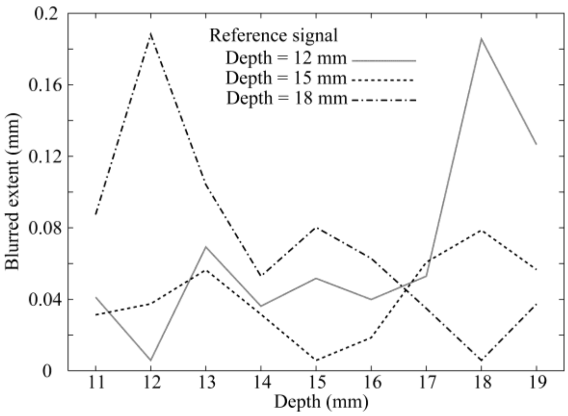

Figure 4. Blurred extent of FDI images of horizontal interfaces at depths of 11 to 19 mm. The FDI imaging method employs one of the echoes returned from interfaces at depths of 12, 15 and 18 mm as the reference signal.

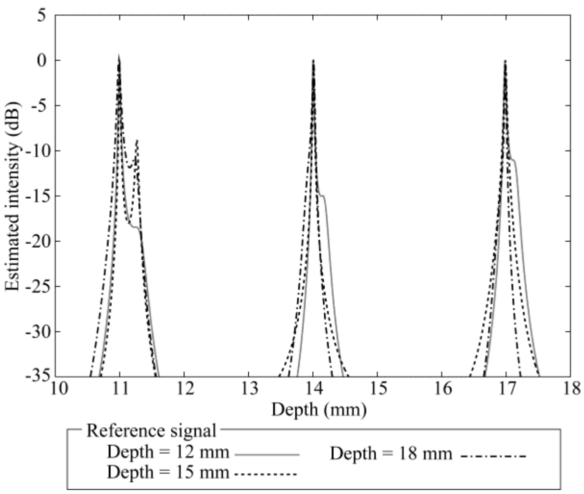

Figure 5. Estimated intensity acquired using the FDI imaging method, where the depths of the reference signals are 12, 15 and 18 mm. Horizontal interfaces exist at depths of 11, 14 and 17 mm.

The high-range-resolution imaging of carotid arterial walls should improve the accuracy in measuring carotid stiffness and carotid intima-media thickness (CIMT). Therefore, we focus on the depiction of anterior and posterior carotid arterial walls. We divide the ROI in a human carotid artery into two sub-ROIs, where each sub-ROI includes a carotid arterial wall. The depths of the reference signals for the anterior and posterior sub-ROIs are 12 and 18 mm, respectively. In the experimental study, we employ the reference compound technique for stabilization [12].

III. RESULTS

First, we investigated the efficiency of RDP in a simulation study. Fig. 6 shows the estimated intensity acquired using a conventional FDI imaging method and the FDI imaging method with RDP, where horizontal interfaces are located at depths of 11, 12, 13, 17, 18 and 19 mm. The employment of RDP succeeds in acquiring sharp images and suppressing the appearance of false peaks. This result shows the high potential of the FDI imaging method with RDP in carotid artery imaging.

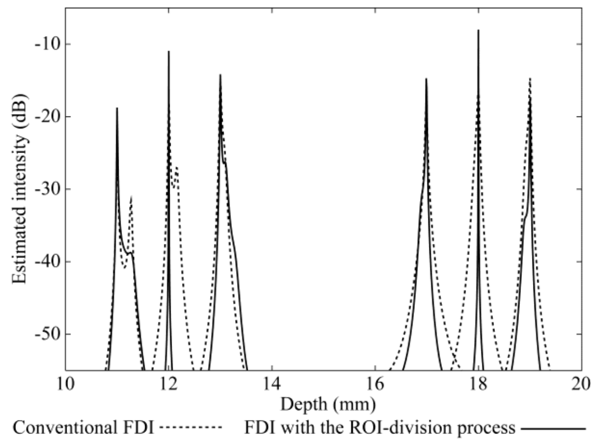

Figure 6. Estimated intensity acquired using a conventional FDI imaging method and the FDI imaging method using the ROI-division process. A single interface exists at depths of 11, 12, 13, 17, 18 and 19 mm.

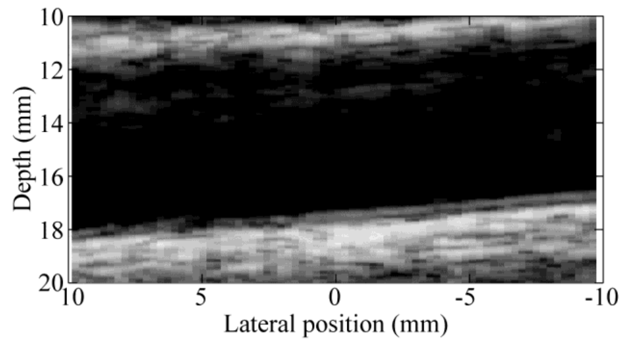

Figure 7. Ultrasound images of an in-vivo human carotid artery acquired using a conventional B-mode imaging method.

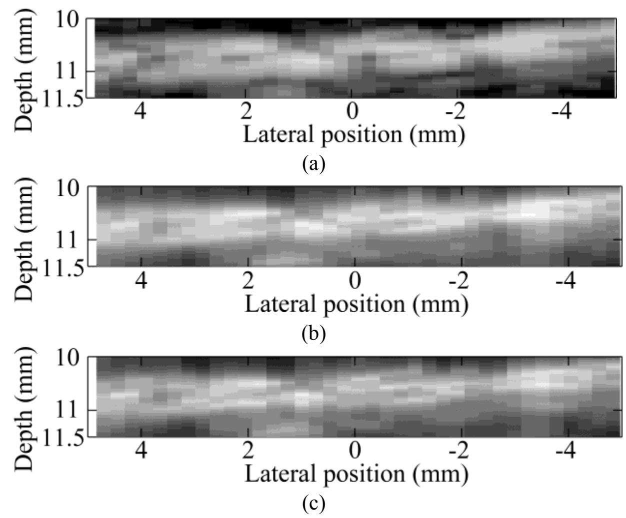

Figure 8. Magnified ultrasound images of an in-vivo human carotid artery at the position of the anterior wall acquired (a) using a conventional B-mode imaging method, (b) a conventional FDI imaging method, and (c) the FDI imaging method with the ROI-division process.

We applied the FDI imaging method with the proposed technique to the raw data from a human carotid artery in a living normal subject. Figs. 7 and 8 show the ultrasound images of a human carotid artery acquired using a

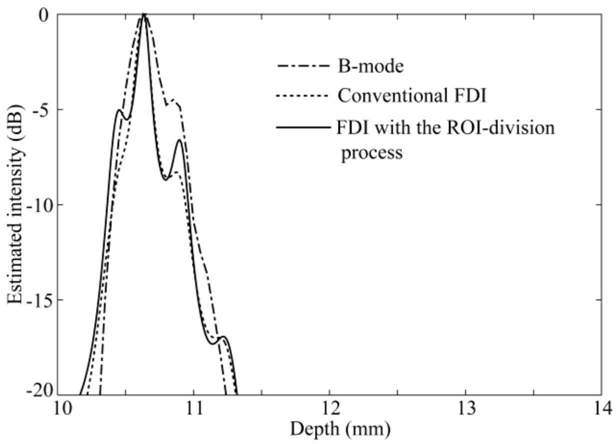

(a)

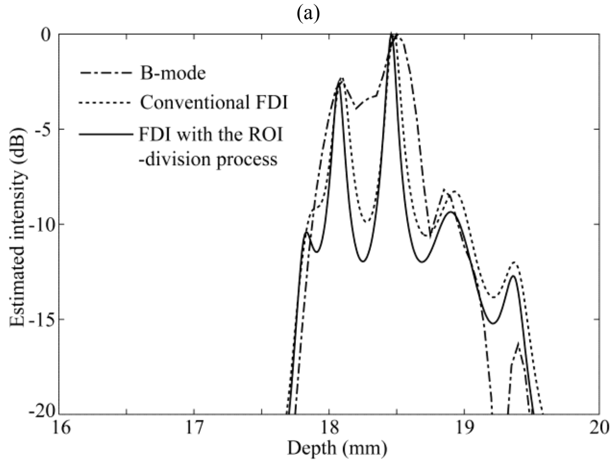

(b)

Figure 9. Estimated intensity in a scan line at the position of (a) the anterior and (b) posterior walls of a human carotid artery acquired using a conventional B-mode imaging method, a conventional FDI imaging method, and the FDI imaging method with the ROI-division process. Each esitimated intensity is normalized by its peak intensity.

conventional B-mode imaging method, a conventional FDI imaging method, and the FDI imaging method with RDP. The three imaging methods were applied to the same raw data obtained using a commercial US devise with a 7.5 MHz linear array probe. Fig. 9 shows the estimated intensity in a scan line at the position of the anterior and posterior carotid arterial walls, where each echo intensity is normalized by its peak intensity. Both the conventional FDI imaging method and the FDI imaging method with RDP succeeds in acquiring high-range-resolution images as compared with the conventional B-mode images. The FDI imaging method with RDP depicts a high-contrast image as compared with the conventional FDI imaging method. The average blurred extent of the anterior carotid arterial wall acquired using a B-mode imaging method, a conventional FDI imaging method and the FDI imaging method with the proposed process are 0.202, 0.132 and 0.0884 mm, respectively. Those of the posterior wall acquired by the three methods are 0.335, 0.242 and 0.136 mm, respectively. In this investigation, we used the half-power widths of the peak lobes in 15 scan lines. These results are consistent with the simulation study, indicating the efficiency of the proposed process in improving the image quality acquired using the FDI imaging method.

IV. Conclusion

In the current study, we report that varying target depth causes the deterioration of the image quality acquired using the FDI imaging method. We propose a process that divides a ROI into multiple sub-ROIs to suppress the variation of the echo waveform caused by varying target depth. The simulation and experimental studies indicate the efficiency of the proposed process in suppressing the deterioration in image quality. We believe that the FDI imaging method with the proposed ROI-division process has the potential to improve the accuracy of vascular ultrasound in measuring the diameter of a carotid artery and the thickness of a carotid arterial wall thickness; these are important indicators in assessing the risk of cardiovascular diseases.

References

[1] E. G. Grant, C. B. Benson, G. L. Moneta, A. V. Alexandrov, J.D. Baker, E. I. Bluth, B. A. Carroll, M. Eliasziw, J. Gocke, B. S. Hertzberg, S. Katanick, L. Needleman, J. Pellerito, J. F. Polak, K. S. Rholl, D. L. Wooster, and R. E. Zierler, "Carotid artery stenosis: Gray-scale and Doppler US diagnosis—society of radiologists in ultrasound consensus conference," *Radiology*, vol. 229, no. 2, pp. 340–346, Nov. 2003.

[2] D. H. O'Leary and M. L. Bots, "Imaging of atherosclerosis: carotid intima-media thickness," *Eur Heart J*, vol. 31, no. 14, pp. 1682–1689, July 2010.

[3] J. Capon, "High resolution frequency-wavenumber spectrum analysis," *Proc. IEEE*, vol. 58, no. 8, pp. 1408–1418, Aug. 1969.

[4] O. L. Frost, "An algorithm for linear constrained adaptive array processing," *Proc. IEEE*, vol. 60, no. 8, pp. 926–935, Aug. 1972.

[5] J. A. Mann and W. F. Walker, "A constrained adaptive beamformer for medical ultrasound: initial results," in *Proc. IEEE Ultrason. Symp*., 2002, pp. 1807–1810.

[6] J. A. Mann and W. F. Walker, "Constrained adaptive beamforming: point and contrast resolution," in *Proc. SPIE*, 2003, pp. 12–23.

[7] J. F. Synnevåg, A. Austeng, and S. Holm, "Benefits of minimum-variance beamforming in medical ultrasound imaging," *IEEE Trans. Ultrason. Ferroelectr. Freq. Control*, vol. 56, no. 9, pp. 1868–1879, Sep. 2009.

[8] J. F. Synnevåg, A. Austeng, and S. Holm, "A low-complexity data-dependent beamformer," *IEEE Trans. Ultrason. Ferroelectr. Freq. Control*, vol. 57, no. 2, pp. 281–289, Feb. 2010.

[9] H. Taki, K. Taki, T. Sakamoto, M. Yamakawa, T. Shiina, and T. Sato, "High range resolution medical acoustic vascular imaging with frequency domain interferometry," in *Proc. IEEE EMBC*, 2010, pp. 5298–5301.

[10] H. Taki, K. Taki, T. Sakamoto, M. Yamakawa, T. Shiina, M. Kudo, and T. Sato, "High range resolution ultrasonographic vascular imaging using frequency domain interferometry with the Capon method," *IEEE Trans. Med. Imaging*, vol. 31, no. 2, pp. 417–429, Feb. 2012.

[11] H. Taki, T. Sakamoto, M. Yamakawa, T. Shiina, and T. Sato, "High resolution ultrasound imaging using frequency domain interferometry―suppression of interference using adaptive frequency averaging―," *IEEJ Trans. Electron. Inf. Syst*., vol. 132, no.10, pp. 1552–1557, Oct., 2012.

[12] H. Taki, T. Sakamoto, K. Taki, M. Yamakawa, T. Shiina, M. Kudo, and T. Sato, "High range resolution ultrasound imaging of a human carotid artery using frequency domain interferometry," in *Proc. IEEE Ultrasonics Symp*, 2011, pp. 2201–2204.